

The Effects of Viscosity on the Hydrodynamic Properties of Bodies in a Free Surface

R. W. Yeung and R. K. M. Seah

Mechanical Engineering & Ocean Engineering
University of California at Berkeley
Berkeley, California 94720-1740, USA

1 Background

Classical analysis of problems of floating bodies in waves relies often on the inviscid-fluid assumption, which has provided useful engineering results. However, it is important that one should also assess the effects of viscosity on this simpler means of modeling, or at least assess it in a controlled environment. As is well known, the solution of the viscous-fluid flow problem with a free surface can be quite demanding. Unlike inviscid-fluid flow which can be well treated by a boundary-integral formulation, viscous flow requires one to work with the entire flow field. Field discretization is hence often necessary, and can be cumbersome with mesh-generation grid-convergence issues that need to be addressed. Further, the complication that goes with accommodating the unknown moving free-surface boundary must be handled.

The advent of an intermediate but efficient solution methodology called Free-Surface Random-Vortex Method (FSRVM) for modeling vortical flows in a wavy environment makes such efforts of assessment more manageable. The FSRVM method was outlined in Yeung *et al.* (1998). An overview of its validations and wide-ranging capabilities was given in the review article of Yeung (2002). This is a boundary-integral method that merges inviscid-fluid modeling with a grid-free solution of the Navier-Stokes equation.

In this paper, this method for viscous free-surface flow is used to investigate the effects of viscosity on two categories of hydrodynamic problems:

A swaying cylinder submerged under a free surface.

The analytical solution of this problem was carried out skillfully by Ogilve (1963), who was the first to discover the possible existence of negative added mass for heave motion. More recently, a linearized Navier-Stokes solution of this problem was developed by Yeung & Wu (1991). They provided the necessary viscous-fluid Green functions of the Navier-Stokes equations with the convective terms neglected, but the effects of free-surface included. This was essentially a free-surface “vorticity-diffusion” theory, which marked the beginning of the many recent efforts to model viscous effects on free-surface flows. The solution of FSRVM to be shown below will address the nonlinear effects as a result of vorticity generated by body motion.

Resonant hydrodynamics of twin bodies. Analysis of pairs of surface-piercing heaving circular cylinders was performed by Wang and Wahab (1971). It showed the occurrence of a multitude of “moonpool modes” of oscillation in the gap between the twin bodies. At such resonant modes, the added mass and damping vary rapidly. The joint bodies experience substantial inertia and damping at the same time. The occurrence of these modes is marked by a sign change in the added mass coefficient. This behavior is quite a contrast to the so-called “trapped modes” recently investigated by McIver (1996) and others, in a manner consistent with John’s (1950) original non-uniqueness proof for a single body. John established that the condition for the unique (frequency-domain) solution to a class of single surface-piercing bodies requires that any vertical line emerging from the body should not intersect the free surface. In the frequency domain, McIver obtained specific shapes of a pair of bodies which satisfy homogeneous boundary conditions everywhere. Newman (1999) extended the problem to axisymmetric three-dimensional toroidal bodies. The occurrence of trapped modes is marked by large hydrodynamic inertia but with no radiating waves. We will focus our time-domain solution by FSRVM on the latter case of twin bodies. The more conventional “resonant” event is addressed elsewhere.

2 The FSRVM Solution

FSRVM uses a complex-variable boundary-integral method to solve the two-dimensional problem. It is based on an Eulerian-Lagrangian description and is particularly efficient at solving for viscous effects with nonlinear free surface boundary conditions. Briefly, from Yeung *et al.* (1998), let the 2-D computational domain be designated by D , bounded by ∂D , with the body denoted by the total contour ∂D_b , the free surface ∂D_f , and an open boundary ∂D_Σ . We take the Ox axis to be horizontal and the Oy axis vertical. FSRVM uses a formulation of vorticity ξ , which is normal to the Oxy plane and stream function ψ . The governing equations are:

$$D_t \xi = \nu \nabla^2 \xi, \quad \nabla^2 \psi = -\xi, \quad (1)$$

where D_t is the material derivative and ν the kinematic viscosity coefficient.

The vorticity field can be represented by a collection of vortex blobs, whose movement is governed by the (1), which is solved by a two-(fractional) step method: a diffusion step and a convection step. The former is handled by a random-walk algorithm but the latter requires evaluating the complex interaction of the vortex blobs and the boundary ∂D . To model this, we can write $\psi = \psi_h + \psi_v$, where ψ_v is vortical and ψ_h a homogeneous solution. Given that ψ_h satisfies the Laplace's equation, we can introduce a complex potential $\beta_h(z, t) = \phi_h + i\psi_h$, where ϕ_h is the conjugate function (velocity potential) and $z = x + iy$.

The existing knowledge of ψ_v and the solution of β_h will give the velocity field. To find β_h , we use Cauchy's integral theorem to obtain an integral equation to be solved, with either ϕ_h or ψ_h specified on the boundary ∂D :

$$\pi i \beta_h(z) - \oint_{\partial D} \frac{\beta_h(\zeta)}{\zeta - z} d\zeta = 0 \text{ for } z \in \partial D. \quad (2)$$

On the body boundary ∂D_b , the no-leak condition can be shown to yield:

$$\psi_h = -\psi_v + \dot{x}_b \bar{y} - \dot{y}_b \bar{x} - \frac{1}{2} \dot{\alpha} R_o^2 \text{ on } \partial D_b. \quad (3)$$

where \dot{x}_b , \dot{y}_b , and $\dot{\alpha}$ are the rigid-body velocities of the body and $R_o = \sqrt{\bar{x}^2 + \bar{y}^2}$ for a body point with coordinates (\bar{x}, \bar{y}) . If z is on the free surface ∂D_F , the kinematic boundary condition for the complex velocity $w = u - iv$ can be used to advance the location of the free surface, while the dynamic condition can be used to advance ϕ_h :

$$D_t z = w^*(z, t) - \nu_d(z - z_o), \quad (4)$$

$$D_t \phi_h = -D_t \phi_v + \frac{1}{2} w w^* - gy - \nu_d \phi, \quad (5)$$

with $*$ indicating complex conjugate. The damping function ν_d in Eqns. (4) and (5) is trivially zero except in the damping layers, say, $-L < x \leq x_l$ and $L > x \geq x_r$ on the left and right ends of the free surface, and z_o is the initial location of the lead free-surface points of the layers at $t = 0$. The use of damping layers allows a no-disturbance condition be applied on the open boundary ∂D_Σ . Alternative absorbing boundary conditions provided by Clément (1996) are also effective.

After β_h is solved, the important "no-slip" boundary condition on ∂D_b is satisfied by generating vorticity of an opposite sign to nullify the tangential surface velocity from β . The convective movement of the vortex blobs is computed using an $O(N)$ algorithm, which allows long-time simulation possible as the number of vortices, N , increases in time. The diffusion algorithm involves a random walk, as mentioned earlier.

To obtain the forces and moment on the body, we need to solve for $\partial \beta_h / \partial t$, since $\partial \phi_h / \partial t$ is needed in Euler's integral to evaluate the fluid pressure.

$$\frac{p}{\rho} = -\frac{\partial(\phi_h + \phi_v)}{\partial t} - \frac{1}{2} |\nabla \phi|^2 - gy, \quad (6)$$

Thus, an integral equation in parallel to Eqn. (2) has to be set up for $\partial \beta_h / \partial t$. The requisite boundary conditions for

$\partial \phi_h / \partial t$ on ∂D_F are then given by Eqn. (5). On ∂D_b ,

$$\frac{\partial \psi_h}{\partial t} = \dot{x}_b \bar{y} - \dot{y}_b \bar{x} - \frac{1}{2} \dot{\alpha} R_o^2 - \left\{ \frac{\partial \psi_v}{\partial t} + \dot{x}_b v - \dot{y}_b u + \dot{\alpha} [(\dot{x}_b - u)\bar{x} + (\dot{y}_b - v)\bar{y}] \right\}. \quad (7)$$

Once $\partial \beta_h / \partial t$ has been obtained, the pressure, p , is known from (6) and the forces and moments on the body follow directly from integration:

$$[F_1, F_2, M_3] = \int_{\partial D_b} p [n_1, n_2, n_1 y - n_2 x] ds, \quad (8)$$

Note that in the absence of ψ_v , the flow is entirely irrotational. Thus, a fully nonlinear inviscid solution can be recovered using FSRVM by turning off the vorticity generation process.

In the results to follow, the added-mass and damping coefficients associated with a given direction of body motion, e.g., μ_{22} , λ_{22} for heave, are obtained by Fourier-analyzing the time history or forces or moment, using a moving window that has a width of one period of oscillation of the body T . If the flow process is steady, μ_{22} and λ_{22} would not be changing in time. However this is not true in viscous flow. Non-dimensional coefficients, when presented, are normalized by density ρ and \forall , the cross-sectional area of the body profile. Frequency ω is normalized by $\sqrt{g/b}$ where b is a "characteristic beam".

3 Results and Discussion

3.1 Submerged oscillating circular cylinder

A fully submerged circular cylinder of laboratory scale, of diameter $D = 30.5\text{cm}$, is undergoing a sinusoidal, swaying motion of amplitude, A . The depth h from $y = 0$ to center of the cylinder is $0.75D$. This configuration has the known property of negative added mass for heave motion (Ogilvie, 1963) in a range of ω^* , where $\omega^* \equiv \omega \sqrt{D/2g}$ is typically $O(1)$. This property was in fact observed in conventional inviscid-fluid computations as well as in the vorticity-diffusion theory of Yeung & Wu. FSRVM also reproduced this negative added-mass property.

In the present study, the cylinder is subjected to two different sway-motion amplitude to diameter ratios, $A/D = 0.033$ and $A/D = 0.10$, or equivalently, a Keulegan-Carpenter number, $KC \equiv 2\pi A/D = 0.209$ and 0.628 , respectively, with the frequency parameter, ω^* varied from 1.0 to $\sqrt{2}$. The FSRVM computations are compared with those obtained using the frequency-domain method in Yeung and Wu (1991). The specific study corresponds to a "frequency Reynolds number" $R_\omega \equiv g^2/\nu\omega^3$ defined therein varying from 1.63×10^5 to 5.84×10^5 (ν taken at a standard value). In this range of values, Yeung and Wu argued that under the small-motion assumption, the effect of viscosity is to merely generate a thin shear layer, which would have little overall effects on the inviscid-fluid coefficients. Figure 1 shows the typical time histories of the sway force, heave force, and roll moment of the submerged circular cylinder under the prescribed sway motion of $A/D = 0.033$ with $\omega^{*2} = 1.00$. The sway-force time history is relatively smooth and continuous, as compared

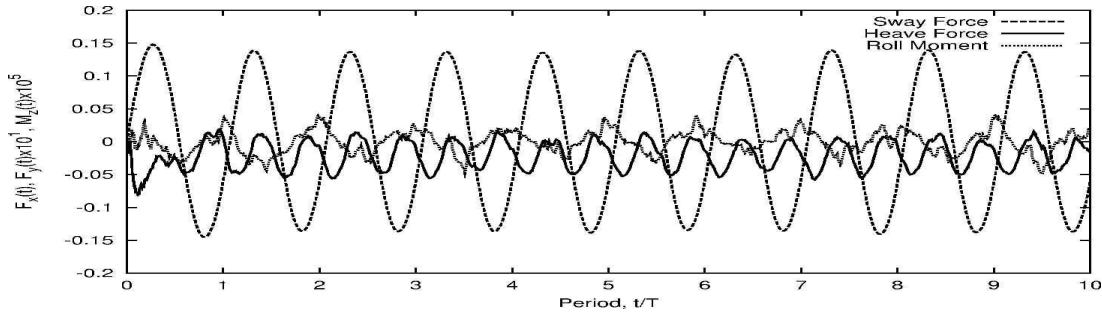


Figure 1: Time history of Sway, heave forces, and roll moment, $\omega^* = 1.00$, $A/D = 0.033$ ($KC = 0.209$).

to the heave force and roll moment time histories, which have significant fluctuations. The heave force has approximately twice the frequency of the sway force, which is a consequence of the nonlinear body boundary condition. Figures 2 and 3 show the added-mass and linear damping coefficients of the two cases of $A/D = 0.033$ and $A/D = 0.10$, as functions of ω^{*2} . Also plotted are the results obtained from the vorticity-diffusion theory of Yeung and Wu (1991). While both cases have similar trends of added masses, the FSRVM values are higher than those from the vorticity-diffusion theory. This may be interpreted as the effect of including convection in the FSRVM method. The difference between the two solutions diminishes as the frequency increases. Interestingly, for damping, all three sets of results seem to be in general agreement, especially at higher frequencies. It is noteworthy that in the two sets of results of FSRVM, the case with the lower amplitude ratio, $A/D = 0.033$, has a higher linear damping coefficient. The Yeung & Wu results appear to overpredict the linear damping across the entire frequency range studied, albeit converge at higher frequencies to the case of low A/D ratio of FSRVM. Figures 4 and 5 show the differences in the vortex blob distribution around the cylinder at the typical frequency, $\omega^* = \sqrt{2.0}$. The dispersion distance of the vortex blobs for the smaller amplitude ratio case is clearly lower than that of the higher amplitude-ratio case. With the existence of vorticity, the equivalent bodies of the two cases are enlarged, especially in the direction parallel to the x-axis. These elongated, equivalent bodies would also tend to generate less waves on the free surface than the original circle. Since lower frequency would allow a longer duration for viscous diffusion to take place, an elongated equivalent body would hence yield *smaller* damping coefficients (Figure 3) when compared with the circular shape in the Yeung & Wu solution. Further, with a larger amplitude, it would be natural for the case of $A/D = 0.10$ to assume a longer equivalent body, and thus lower damping. As the frequency increases, the damping of the viscous cases converge to that of the diffusion theory as the diffusion time diminishes. Higher frequency would also mean a higher Reynolds number, with inertial effects beginning to dominate. A more general test of the effects of convection can be done by carrying out computations for $A/D = O(10)$.

3.2 Twin Bodies with Trapped Modes

The existence of trapped modes depend on the shapes of the bodies. The ‘‘McIver profile’’ was generated by plotting

streamlines generated using the results of McIver (1996). In this nonlinear study, the nonlinear solution requires a definition of the body above $y = 0$ which we obtained by extending the generated streamline above $y = 0$. The first trapped mode is located at $\omega^* = 1.38$, where b is the characteristic beam defined as the submerged area of one body divided by its draft. With the generator of vorticity turned off, and at an ‘‘absolutely small’’ amplitude of motion, $A/b = -0.00043$, where one could argue that linearized theory remains valid, FSRVM produces the time history of wave elevation in the gap and beyond the body (at $x/b = 9$) as shown in Figure 6. If the bodies are given vertical motion at this frequency, the solution was expected to grow without bound (McIver *et al.*, 2002). Instead, we observed bounded free surface elevations. Note that, in magnitude, the waves outside are only $O(10^{-2})$ of that in the gap, a characteristic of trapped-mode behavior. An examination of the hydrodynamic coefficients in Figure 8 reveal a local minimum in damping and a local maximum in added mass close to this trapped-mode frequency.

With viscosity present, but retaining the small-motion assumption, the shape of the profile is effectively unaltered by the shear layers around most of the body except in the region near the moonpool. Even so, this is sufficient to increase radiating wave heights (Figure 7) and change the behaviour of the moonpool. As a matter of fact, the vorticity in the convergent gap between the twin bodies (Figure 9) accentuates the motions since it increases the constriction. Figure 8 shows a distinct change in frequency where the minimum damping coefficient occurs. The region to the right of the black vertical lines display resonant behaviour where coefficients cannot be accurately obtained.

4 References

- Clément, A. (1996). *J. Comp. Phys.*, **126**, pp. 139-151.
- McIver, M. (1996). *J. Fluid Mech.*, **315** pp. 257-266.
- McIver, P., McIver, M. and Zhang, J. (2002). *17th IWWWFB*, Cambridge, UK, pp. 119-122
- Newman J. N. (1999). *J. Engrg. Math.*, **35**, pp. 135-147.
- Ogilvie, T. F. (1963). *J. Fluid Mech.*, **16**, pp. 451-472.
- Wang, S. and Wahab, E. (1971). *J. Ship Research*, **15**, No. 1, pp. 33-48.
- Yeung, R. W. and Wu, C.-F. (1991). *ASME J. Offshore Mech. and Arctic Engrg.*, **113**, pp. 334-343.
- Yeung, R. W., Liao S.-W., and Roddier D. (1998). *Int'l J. Offshore and Polar Engrg.*, **8**, No. 4, pp. 241-250.
- Yeung, R. W. (2002). *Proc. of 12th Int'l Offshore and Polar Engrg Conference*, Kitakyushu, Japan, vol. 2, pp. 1-11.

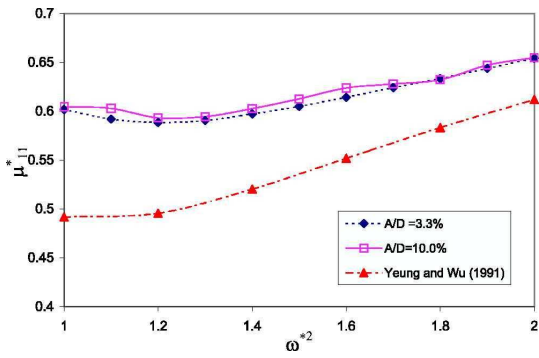


Figure 2: Added mass coefficient versus frequency, $A/D = 0.033, 0.10$ ($KC = 0.209, 0.628$).

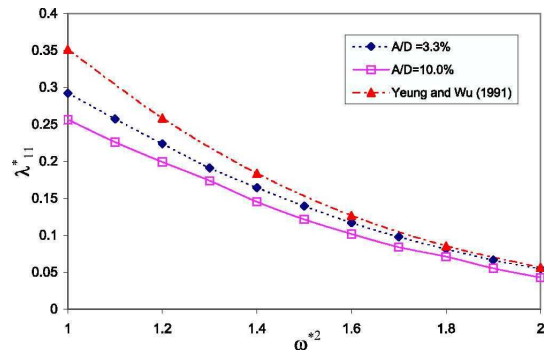


Figure 3: Linear damping coefficient versus frequency, $A/D = 0.033, 0.10$ ($KC = 0.209, 0.628$).

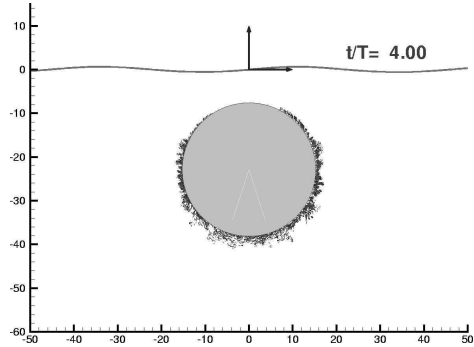


Figure 4: Vortex Blob plots for $A/D = 0.033$ and $\omega^* = \sqrt{2}$.

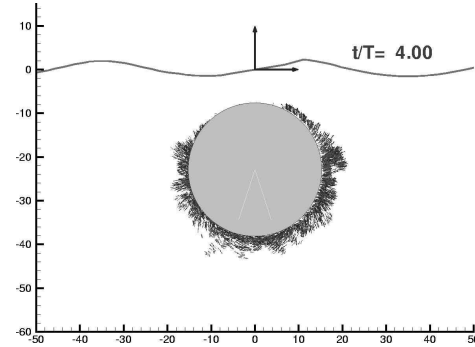


Figure 5: Vortex Blob plots for $A/D = 0.10$ and $\omega^* = \sqrt{2}$.

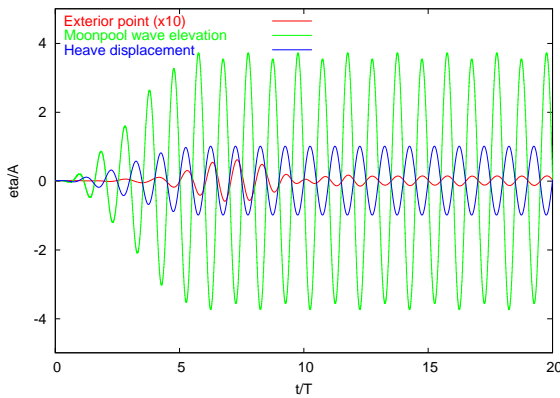


Figure 6: Wave Elevation at $x = 0$ and external location, $\omega^* = 1.38$, inviscid case.

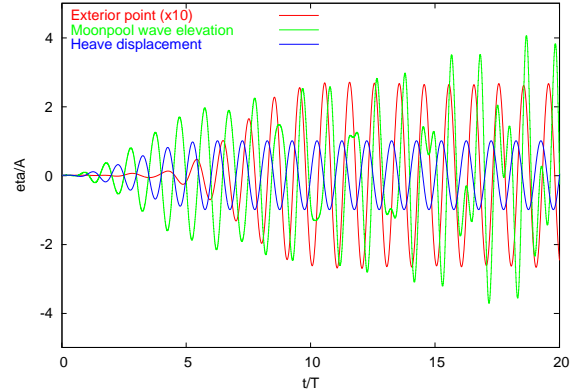


Figure 7: Wave Elevation at $x = 0$ and external location, $\omega^* = 1.38$, viscous case.

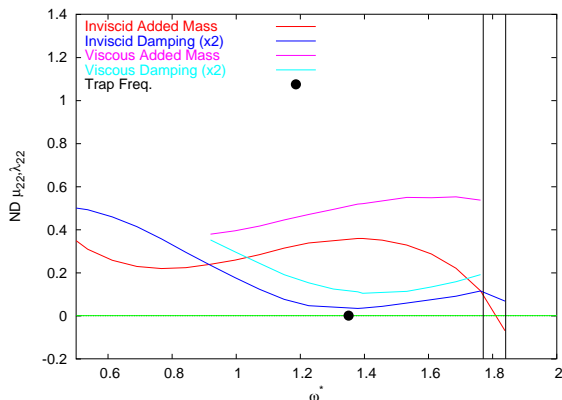


Figure 8: Non-dimensional Added Mass and Damping Coefficients versus Frequency.

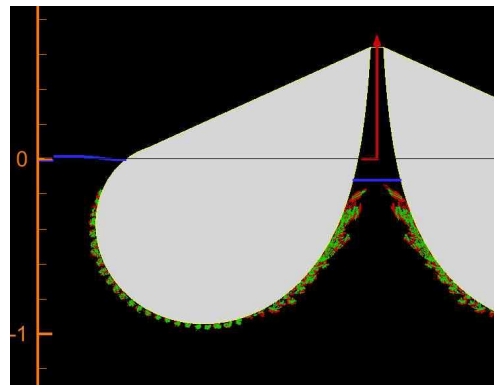


Figure 9: Vortex-blob structure around body profile at trapped mode.

Discusser: Q. Ma

You have given results associated with the sway motion of a submerged cylinder with amplitude being up to 10 % of its diameter. Could I ask what will happen if the amplitude is larger than that ?

Author's reply:

For this configuration, if the amplitude is increased beyond 10 %, the simulation produces breaking waves. The current version of the algorithm is unable to handle breaking waves and the resulting shortened force time history would be inadequate to obtain meaningful Fourier values for the hydrodynamic coefficients.

Discusser: M. Mc. Iver

In the twin floating cylinder case would you expect to find an extra 'resonant mode' as well as the trapped mode (analytically) in the linear case? This would be quite a surprise as I would expect the trapped mode to coincide with the lowest moon-pool resonance.

Author's reply:

Wang and Wahab (1971, cited in our work) studied analytically the heaving behavior of twin circular cylinders. They showed the existence of a family of 'resonant' modes, with singular hydrodynamic coefficients, dependent on the cylinder geometry and separation. It is reasonable to expect that the current cylinders would also have similar behavior in addition to the 'trapped mode' oscillation. The behavior around these two type of frequencies are different.